BOEING SCIENTIFIC RESEARCH LABORATORIES DOCUMENT D1-82-0742

BOEING

SCIENTIFIC RESEARCH LABORATORIES

Undulance and Turbulence in Stably Stratified Media

Yih-Ho Pao

FLIGHT SCIENCES LABORATORY AUGUST 1968

D1-82-0742

BOEING SCIENTIFIC RESEARCH LABORATORIES

Flight Sciences Laboratory

UNDULANCE AND TURBULENCE IN STABLY STRATIFIED MEDIA

by

Yih-Ho Pao

August 1968

BLANK PAGE

UNDULANCE AND TURBULENCE IN STABLY STRATIFIED MEDIA

Yih-Ho Pao
Boeing Scientific Research Laboratories
Seattle, Washington

ABSTRACT

The origin and the structure of undulance and turbulence in stably stratified media are investigated through theoretical reasoning and laboratory experiments. The mechanisms for generating turbulence in stably stratified media are linked with the mechanisms for generating vorticity - shear and stratification. The dual role of stable stratification -- the capability for generating and attenuating turbulence -- is pointed out. The turbulence induced by stable stratification is evidenced in two experimental results: (i) turbulent rotors in the lee of a barrier in a stably stratified fluid, and (ii) the breaking of traveling internal waves on a sloping surface. The ability of stable stratification to generate turbulence is also indicated from an exact solution for an inviscid stably stratified flow past a barrier. The structure of undulance and turbulence in stably stratified media is investigated in a stratified salt water towing tank, with schlieren photographs, quartz-coated hot-film probes, and single electrode conductivity probes. The schlieren photographs show clearly the collapse of a turbulent wake and the attenuation of turbulence by stable stratification. Auto-correlations and -spectra for the streamwise turbulent velocity field and for the turbulent concentration field are obtained from the probe measurements with both analog and digital data processing methods. From the measured correlations and spectra, the combined wave-turbulence behavior is clearly shown, and the turbulence is strongly anisotropic.

This paper prepared for the Boeing Scientific Research Laboratories "Symposium on Clear Air Turbulence and Its Detection", 14-16 August 1968, Seattle, Washington, U.S.A.

1. Introduction

The undulant and the turbulent atmospheric motions in the upper troposphere and in the stratosphere, commonly known as clear air turbulence, are far from being well understood. Theoretical analyses of the flow phenomena can at best yield piecemeal information; the fundamental difficulty is the one common to all nonlinear stochastic processes that there are always more statistical unknowns than equations and thus the problems are statistically indeterminate. Data gathering from airborne measurements have been difficult and expensive. Furthermore, at low frequencies, it is difficult to separate accurately the airplane motion from the atmospheric motion. Existing measurements in the upper troposphere and stratosphere indicate that turbulence are often found in the form of sporadic and isolated patches in strongly stable regions of the atmosphere.

It is the purpose of this investigation to probe the origin and the structure of these undulant and/or turbulent motions in stably stratified media, through theeoretical reasoning and controlled laboratory experiments where the boundary conditions are well defined and the measuring techniques are better established. It is believed that results from laboratory investigation are complimentary to the actual airborne measurements; they will help to isolate the turbulence generating mechanisms and to untangle the structure of turbulence in the upper atmosphere where the air is stably stratified.

This is a part of a series investigations at the Boeing Scientific Research Laboratories on the laminar, transition, and turbulent flows in stably stratified media. (Pao, 1965, a,b,; Pao and Timm, 1966; Timm and Pao, 1966; Graham, 1966; a,b, Pao, 1967, a,b; Graham and Graham, 1967, a,b,

Pao, 1968, a,b,c,d; Pao, Callahan, and Timm, 1968.)

2. Limitations of Laboratory-Simulated Geophysical Flows

Before presenting our experimental results, it is important to clarify some of the limitations of the laboratory-simulated geophysical flows. In general, it is not possible to simulate in the laboratory all the parameters and all the complicated and ever-varying wind and temperature structure in the atmosphere.

To achieve complete similarity between model experiments and atmospheric flows, it is necessary to have (i) geometric similarity, (ii) kinematic similarity, and (iii) dynamic similarity. Complete dynamic similarity is the most difficult to achieve.

In the case of motion in stably stratified atmosphere, the governing dynamic parameters are the Reynolds number Re ($= UL/\nu$) and the Richardson number Ri ($= \frac{g}{\Theta}\frac{d\Theta}{dz} L^2/U^2$), where U is a characteristic velocity, L is a characteristic length, ν is the kinematic viscosity, g is the gravitational acceleration, Θ is the potential density. It is very difficult to simulate both Re and Ri. Generally speaking, in the laboratory it is relatively simple to simulate the proper Richardson number with stratified liquid (atmospheric motions can be treated to a good degree of approximation as incompressible flows) or heated air, but it is very difficult to achieve the huge Reynolds numbers that occur in atmospheric motion. It has been reasoned that variations of the flow (with Reynolds numbers) are small at large Reynolds numbers, and thus the flow is only weakly dependent on the Reynolds number. This argument, although quite logical, has not yet been looked into quantitatively. An attempt was made (Timm and Pao, 1966) to study the Reynolds

number asymptotic behavior under a fixed Richardson number for laboratory simulated mountain waves. The results are inconclusive because of the very limited range of Reynolds numbers attainable with our experimental facility. Therefore, extrapolation of the laboratory results obtained in flows with moderate Reynolds numbers to the atmosphere motion with very large Reynolds numbers, is to be approached with caution. It is only those phenomena which are weakly dependent on the Reynolds number that can be extrapolated.

3. Two Mechanisms for Generating Turbulence in Stably Stratified Media

Turbulence is always associated with strong vorticity fluctuation. These vorticities are generated in the flow when it undergoes transition from laminar to turbulent states. The mechanisms for generating vorticity in stratified media, thus for generating turbulence, can be clearly identified through the vorticity equation for a viscous incompressible stratified fluid:

$$\frac{D\underset{\sim}{\omega}}{Dt} + \nu\nabla\times(\nabla\times\underset{\sim}{\omega}) = (\underset{\sim}{\omega}\cdot\nabla)\underset{\sim}{U} + \rho^{-2}\nabla\rho\times\nabla P \qquad (3.1)$$

Rate of change of vorticity following a fluid parcel	Viscous diffusion of vorticity	Generation of vorticity by shear	Generation of vorticity by stratification

where $\underset{\sim}{\omega}$ is the vorticity; $\underset{\sim}{U}$ is the velocity; ρ is the density; P is the pressure; ν is the kinematic viscosity and is assumed to be a constant (which is a good approximation to many physical problems). From (3.1) there are two mechanisms for generating vorticity in stratified flows: $(\underset{\sim}{\omega}\cdot\nabla)\underset{\sim}{U}$ and $\rho^{-2}\nabla\rho\times\nabla P$. The term $(\underset{\sim}{\omega}\cdot\nabla)\underset{\sim}{U}$ represents the generation of vorticity by convective stretching of vortex lines; this mechanism exists in homogeneous as well as inhomogeneous fluid flows. The term $\rho^{-2}\nabla\rho\times\nabla P$ represents the

generation or extraction of vorticity through interaction of the density and pressure gradients; it is a new mechanism for generating vorticity introduced by stratification. These two mechanisms, which are responsible for the generation of vorticity in stratified media, are thus responsible for the generation of turbulence. The structure of turbulence in stably stratified media is then dependent on the relative magnitude of these two mechanisms. Let us define a parameter γ, where

$$\gamma = \frac{|\rho^{-2}\nabla\rho\times\nabla P|}{|(\underset{\sim}{\omega}\cdot\nabla)\underset{\sim}{U}|} = \frac{\text{vorticity generated by stratification}}{\text{vorticity generated by shear}} . \qquad (3.2)$$

For small γ, turbulence, if present, is mainly induced by shear. For large γ, turbulence is mainly induced by stratification. The shear-induced turbulence is a common phenomenon and needs no further explanation. The turbulence induced by unstable stratification, such as by thermal plumes, is also physically obvious. However, turbulence induced by stable stratification needs further explanation. The stable stratification plays the dual role of generating and attenuating turbulence. The capability of stable stratification to generate and to attenuate turbulence will be discussed in Sections 4 and 5

4. Stable Stratification-Induced Turbulence

4.1 Indication from an inviscid theory

Consider an inviscid two-dimensional stratified fluid flow: (3.1) becomes

$$\frac{D\underset{\sim}{\omega}}{Dt} = \rho^{-2}\nabla\rho\times\nabla P . \qquad (4.1)$$

Thus, stratification is the only mechanism to generate vorticity. Pao (1967) has obtained an exact solution for the steady inviscid two-dimensional non-

diffusive flow of a stably stratified fluid past a barrier in a semi-infinite domain, where $U\rho^{\frac{1}{2}}$ and $d\rho/dz$ are assumed to be constant upstream. The results are expressed in terms of a Richardson number, defined as

$$Ri = \frac{g}{\rho}\left|\frac{d\rho}{dz}\right| L^2/U^2 ,$$

where g is the gravitational acceleration, and L is the barrier height. A flow at moderate Richardson number ($Ri = 0.833$) is shown in Fig. 1, where lee waves are formed behind the barrier. However, at larger Richardson number ($Ri = 1.875$), where the flow is strongly stratified, eddies are formed behind the barrier (Fig. 2). The streamlines in Fig. 1 and Fig. 2 are also isopycnic lines (constant density lines). The streamline patterns (eddies) in Fig. 2 indicate heavier fluid on top of lighter fluid, a condition that is likely to be unstable and to become turbulent.

The solution for stratification-induced eddies was first obtained by Long (1955) for a stratified flow past a barrier in a confined channel. It has been suspected that the presence of eddies is due to the confining upper and lower walls, which could cause the wave resonance phenomenon. However, results in Fig. 2 show the presence of eddies behind a barrier even in an unconfined domain. Furthermore, Long (1955) has demonstrated experimentally the existence of these stratification-induced eddies behind a barrier in a relatively shallow fluid.

4.2 Evidence from laboratory experiments - 1. Lee waves and rotors behind a barrier

In this section we shall demonstrate from our experimental results the presence of the stratification-induced turbulent eddies (they are called the "rotors" in some meteorology literature) behind a barrier in a stably strati-

fied flow. The results are obtained in a deeper (compared with that of Long, 1955) towing tank, such that the top free surface effect is small. A two-dimensional wedge resting on a flat plate is used as a model for a mountain ridge (Fig. 3). The wedge is an equilateral triangle and is 2 inches high, with a 30 degree apex angle. The flat plate is 20 inches long. The wedge is resting at the middle of the plate. The model is towed horizontally at constant speed U in a tank of stably stratified salt water with constant density gradient. The tank is 9.5 feet long, 16 inches wide, and 20 inches high (Fig. 4). Fine aluminum powders are used as tracers, illuminated with a sheet of light, 1/4 inch thick and 4 feet wide. The light illuminates the middle portion of the tank and shines from above. A 70 mm camera is traversed at the model speed on a lathe bed parallel to the tank. For a more detailed description of the experimental facility and the flow visualization technique, the reader is referred to a related report (Pao, 1965-1967).

A stably stratified flow over the model ridge is shown in Fig. 5, where $Ri = 13$ and $Re = 914$. Fig. 5 shows : (i) the upstream blocking effect -- the flow in front of the model is slowed down, (ii) the Chinook effect -- strong wind rushes down the back slope, (iii) the lee waves, and (iv) the turbulent rotor -- a turbulent eddy is formed in the lee but away from the barrier, and thus it is induced by stratification and not by boundary layer separation (shear) at the barrier. This shows turbulence induced by stable stratification. To permit comparison of the difference between shear-induced and stratification-induced eddies, a shear-induced eddy caused by boundary layer separation behind a barrier in a homogeneous fluid is shown in Fig. 6.

4.3 Evidence from laboratory experiments - 2. Breaking of internal waves

It has been reasoned that, in stably stratified media, a train of internal waves approaching a sloping sea bed or a sloping land surface may break into turbulence. The breaking of internal waves was proposed (e.g., Phillips, 1966; Long, 1968, among others) as the main mechanism for generation of clear air turbulence.

We have generated in the laboratory a train of internal waves approaching a sloping surface in a stably stratified two fluid system. Fig. 7 shows the internal wave approaching the sloping surface. Fig. 8 shows the internal wave breaking into turbulence. This is another example of stratification-induced turbulence.

The breaking of internal waves on the sloping surface is currently being investigated in detail. The results will be reported with M. Hall in the near future.

It should be noted that the turbulent rotors described in Section 4.2 can be regarded as the breaking of stationary internal waves.

5. Structure of Turbulence in Stably Stratified Media

The structure of turbulence in stably stratified media will depend strongly on the generating mechanisms -- whether it is induced by shear or by stratification, or by both. In what follows, measurements of a shear-induced turbulence in stably stratified salt water will be presented.

5.1 The experiments and data processing

A circular cylinder is towed horizontally at constant speed in a tank of stably stratified salt water with constant density gradient. The tank is 35 feet long, 12 inches wide, and 30 inches high (Fig. 9).* The cylinder is

---

*The author is indebted to Messrs. B. A. Thomas, H. E. Harding, and L. A. Wilson for designing and constructing the towing tank system.

a 3/4 inch (diameter) rod and is neutrally buoyant. It is towed by tightly stretched nylon-coated stainless steel cables (Fig. 10). An air-lubricated probe transport (Fig. 11), mounted with Thermo-Systems quartz-coated hot-film probes and single electrode conductivity probes (similar to those of Gibson and Schwartz, 1963), is towed behind and at the same speed as the circular cylinder. The hot-film probes are used with Thermo-Systems 1010A constant temperature hot-wire anemometers, and the single electrode conductivity probes are driven by Tektronics 3C66 carrier amplifiers. A hot-film probe and a single electrode conductivity probe are placed side-by-side at the wake axis. Another pair are placed 1.5 inches off the wake axis (Fig. 12). The output from the constant temperature hot-wire anemometers and from the Tektronics 3C66 carrier amplifiers is recorded on a 14-channel Ampex CP-100 FM magnetic tape recorder at 15 ips tape speed.* The instruments are shown in Fig. 13.

The signals from the analog tape are processed by both analog and digital methods. For the analog data processing, the signals are re-recorded on loop tapes. The loops are sent to a readout device connected to a Technical Product Wave Analyzer system for spectral analyses,** and to a Princeton Applied Research Laboratory Correlator to obtain auto-correlations. A digital data processing method is developed later, using the Cooley-Tukey fast Fourier transform algorithm (Cooley et al, 1967).*** The analog data are converted to digital form with the Data Technology System Analog-to-

---

* The author is indebted to Mr. G. Bruce for lending the tape recorder and for his operation instructions.

** The author wishes to thank Mr. M. M. Mitchell for the spectral analyses.

*** The author is indebted to Messrs. S. D. Hansen and W. C. Cook for writing the computer program.

Digital Converter.* The digital data are fed into a Univac 1108 computer. The computer output is sent to an SC-4020 printer-plotter. The data processing method is now being changed to direct on-line data processing with an IBM 360-44 computer system.

In addition to the probe measurements, shadowgraph pictures and 16 mm movies are taken to help visualize the flow and identify the region of the turbulent wake.

5.2 The shadowgraph results

As pointed out at the beginning of Secti ı 5, this section is mainly concerned with shear-induced turbulence in stably stratified fluid. The turbulence region begins immediately behind the cylinder. This is quite obvious from the shadowgraph picture in the near wake (Fig. 14). The wake in a stratified fluid is narrower than that in homogeneous fluid. It decays rapidly downstream. Shadowgraph pictures in the far wake (Fig. 15) show that the turbulence is very weak there. These shadowgraph pictures (Figs. 14 and 15) show that stable stratification is an effective mechanism to attenuate turbulence. A phenomenon we have observed in the shadowgraph but which does not present itself clearly in the picture is the strong undulating motion of the turbulent and the nonturbulent interface. This phenomenon can be seen clearly in a 16mm movie film. It is evident from these observations that turbulence in stably stratified fluid is a combined wave-turbulence phenomenon, i.e., undulance and turbulence. This statement will be further substantiated with our probe measurements.

---

* The author is indebted to Mr. R. Miller for lending the DTS system and for his operation instructions.

5.3 Streamwise turbulent velocity spectra and auto-correlations

The attenuation of turbulence by stable stratification is further demonstrated with the spectra of streamwise turbulent velocity on wake axis at 48 diameters downstream of the circular cylinder. Spectra measurements are made in tap water and in stable stratified salt water, respectively, with the same hot-film sensitivity. The results are compared in Fig. 16, and they show clearly the attenuation of turbulence by stable stratification. Webster (1964) observed the fast decay of turbulence intensity behind a nonuniformly heated grid in a wind tunnel, where the heating at the grid increases with height, (thus the fluid is stably stratified,).

It should be noted that the measured streamwise velocity spectral behavior in stably stratified fluids do not differ markedly (except for the lower intensity) from that in homogeneous fluids. The same remark applies to the streamwise velocity auto-correlation. A streamwise turbulent velocity auto-correlation in a stably stratified is shown in Fig. 17. It does not differ significantly from that in the homogeneous wake. The wave-like behavior cannot be detected from either streamwise velocity spectra or auto-correlations.

The Reynolds numbers of our flows are not high enough for investigation of spectral behavior at the buoyancy subrange.

5.4 Turbulent concentration spectra and auto-correlations

The concentration measurements at the wake axis with the single electrode conductivity probes do show strongly the wave-turbulence phenomena, which can be identified through either the spectra or the auto-correlations. The concentration spectrum usually has a single peak (Fig. 18) and the auto-correlation usually has an identifiable wave frequency (Fig. 19).

In this section we have presented some of the preliminary results for wake turbulence in a stably stratified fluid, which is a type of shear-induced turbulence. We have demonstrated, through the concentration spectra and auto-correlations, the combined wave-turbulence behavior. These phenomena have been observed by Reiter and Burns (1966) from their airborne measurements of clear air turbulence in the upper troposphere, although detailed information on meteorological conditions was lacking. The wave-turbulence phenomena are also obvious from the recent HICAT measurements in the stratosphere (Crooks, Hobits, and Prophet, 1967) with a U-2 airplane. Our work on wake turbulence is continuing with investigation of the turbulent structure in the entire wake and in the intermittent regions, and spectral behavior at low frequencies.

ACKNOWLEDGMENTS

The author wishes to thank Messrs. M. E. Callahan and R. L. Carlsen for their assistance. He wishes also to thank Messrs. G. K. Timm, M. Forster, and R. A. Cruz, who helped during the initial stage of this investigation.

REFERENCES

Cooley, J. W., Lewis, P.A.W., and Welch, P. D., 1967: The fast Fourier transform algorithm and its applications. IBM Research Paper RC 1743.

Crooks, W. M., Hoblit, F. M., and Prophet, D. T., 1967: Project HICAT - An investigation of high altitude clear air turbulence, Vol, 1, 2, and 3. Air Force Flight Dynamics Laboratory, Wright-Patterson AFB. Document AFFDL-TR-67-123.

Gibson, C. H., and Schwarz, W. H., 1963: Detection of conductivity fluctuations in a turbulent flow field. J. Fluid Mechanics 16, 357-364.

Graham, E. W., 1966a: The two-dimensional flow of an inviscid density-stratified liquid past a slender body. Boeing Document D1-82-0550.

Graham, E. W., and Graham, B. B., 1966b: Further notes on the two-dimensional flow of an inviscid density-stratified liquid past a slender body. Boeing Document D1-82-0591.

Graham, E. W., and Graham, B. B., 1967a: The effect of Froude number on the two-dimensional flow of an inviscid density-stratified liquid past a slender body. Boeing Document D1-82-0614.

Graham, E. W., and Graham, B. B., 1967b: The effect of a free surface on the two-dimensional flow of an inviscid density-stratified liquid past a slender body. Boeing Document D1-82-0664.

Long, R. R., 1955: Some aspects of flow of stratified fluids III. Continuous density gradients. Tellus 7, 341.

Long, R. R., 1968: Vertical velocities in clear air turbulence. Boeing Document D1-82-0738.

Pao, Yih-Ho, 1965a: Structure of turbulent velocity and scalar fields at large wavenumbers. Phys. Fluids 8 (6), 1063. Boeing Document D1-82-0369.

Pao, Yih-Ho, 1965b: Laminar flow of a stably stratified fluid past a flat plate. Bull. Amer. Phys. Soc. Series II, 8, 426. Boeing Document D1-82-0488, 1967. J. Fluid. Mech. (in the press).

Pao, Yih-Ho, 1967a: Turbulence in stably stratified fluids. Proc. of an IUGG-IUTAM International Symposium on Boundary Layers and Turbulence including Geophysical Applications, Kyoto, Japan, 19-24 September 1966, p. 311. Also Phys. Fluids 10 (9), Part 2, S311.

Pao, Yih-Ho, 1967b: Inviscid flows of stably stratified fluids over barriers. Boeing Document D1-82-0646. Quart. J. Royal Meteor. Soc. (in the press).

Pao, Yih-Ho, 1968a: Transfer of turbulent energy and scalar quantities at large wavenumbers. Phys. Fluids 11 (6), 1371. Boeing Scientific Research Laboratories, Flight Sciences Laboratory Technical Memorandum No. 54.

Pao, Yih-Ho, 1968b: Laminar, transition, and turbulent flows of stably stratified fluids over barriers. Boeing Scientific Research Laboratories, Flight Sciences Laboratory Technical Memorandum No. 55.

Pao, Yih-Ho, 1968c: Laminar flow of a stably stratified fluid past a flat plate. Part 2. Higher-order approximations. Boeing Document (in preparation).

Pao, Yih-Ho, 1968d: Turbulent velocity and scalar fields in stably stratified fluids. To be presented at the Symposium on the Theoretical Problems in Turbulence Research, 9-13 September 1968, University Park, Pennsylvania.

Pao, Yih-Ho, and Timm, G. K., 1966: Flow of a stably stratified fluid past a circular cylinder. Bull. Amer. Phys. Soc. Series II, 11, 721.

Pao, Yih-Ho, Callahan, M. E., and Timm, G. K., 1968: Vortex streets in stably stratified fluids. Boeing Document D1-82-0736.

Phillips, O. M., 1966: The generation of clear-air turbulence by the degradation of internal waves. Proc. Int. Colloq. on the Fine-scale Structure of the Atmosphere and Its Relation to Radio Wave Propagation, Moscow, June 1965.

Reiter, E. R., and Burns, A., 1966: The structure of clear air turbulence derived from "TOPCAT" aircraft measurements. J. Atm. Sci. 23 (2), 206.

Timm, G. K., and Pao, Yih-Ho, 1966: Laboratory simulation of mountain waves. Bull. Amer. Phys. Soc. Series II, 11, 721.

Webster, C.A.G., 1964: An experimental study of turbulence in a density-stratified flow. J. Fluid Mech. 19 (2), 221.

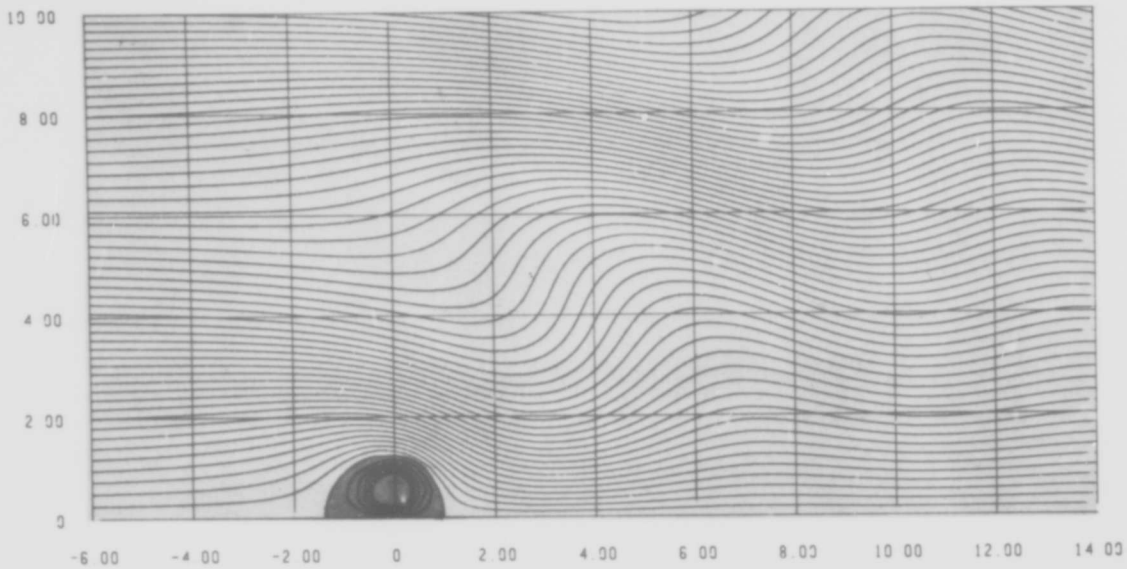

Fig. 1. Lee waves —— an exact solution of an inviscid stably stratified fluid over a barrier (Ri=0.833). The upstream conditions are: $U\rho^{\frac{1}{2}}$ = constant and $d\rho/dz$ = constant. The contour lines are modified streamlines. The characteristic length L=1.

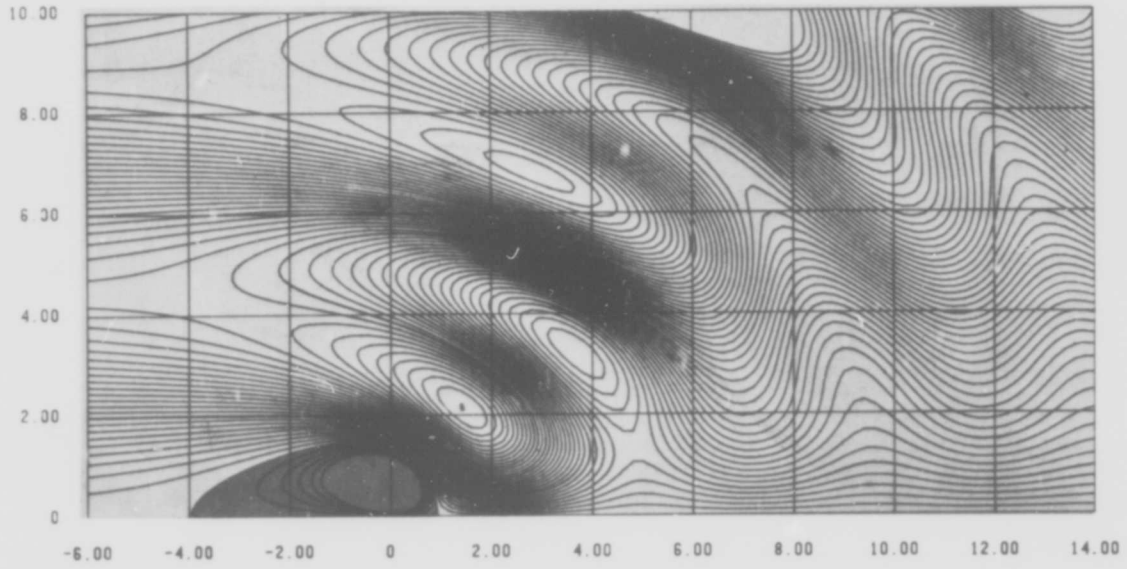

Fig. 2. Rotors —— an exact solution of an inviscid stably stratified fluid over a barrier (Ri=1.875). (See Fig. 2 caption for other details.)

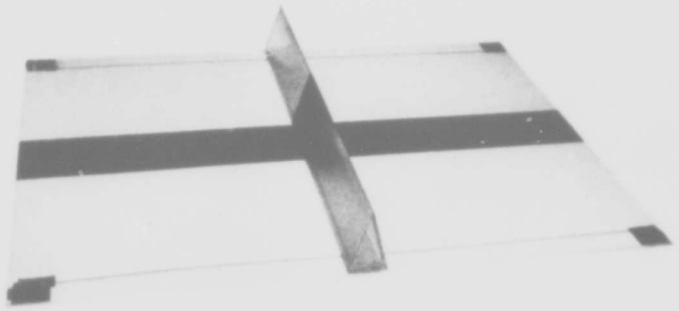

Fig. 3. A mountain ridge model. The wedge is a 2 in. high 30° equal-lateral triangle. The flat plate is a 20 in. long fiber glass sheet. The center black strip is to reduce the light reflected by the flat plate.

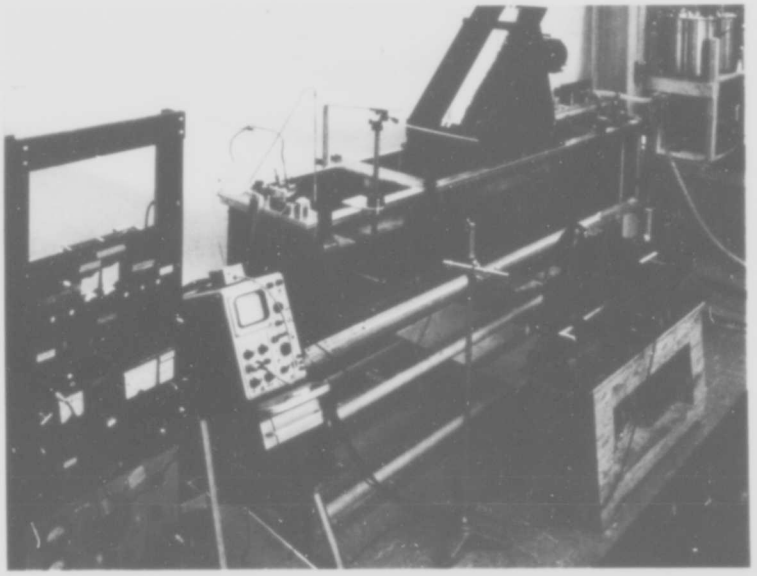

Fig. 4. Towing Tank System A

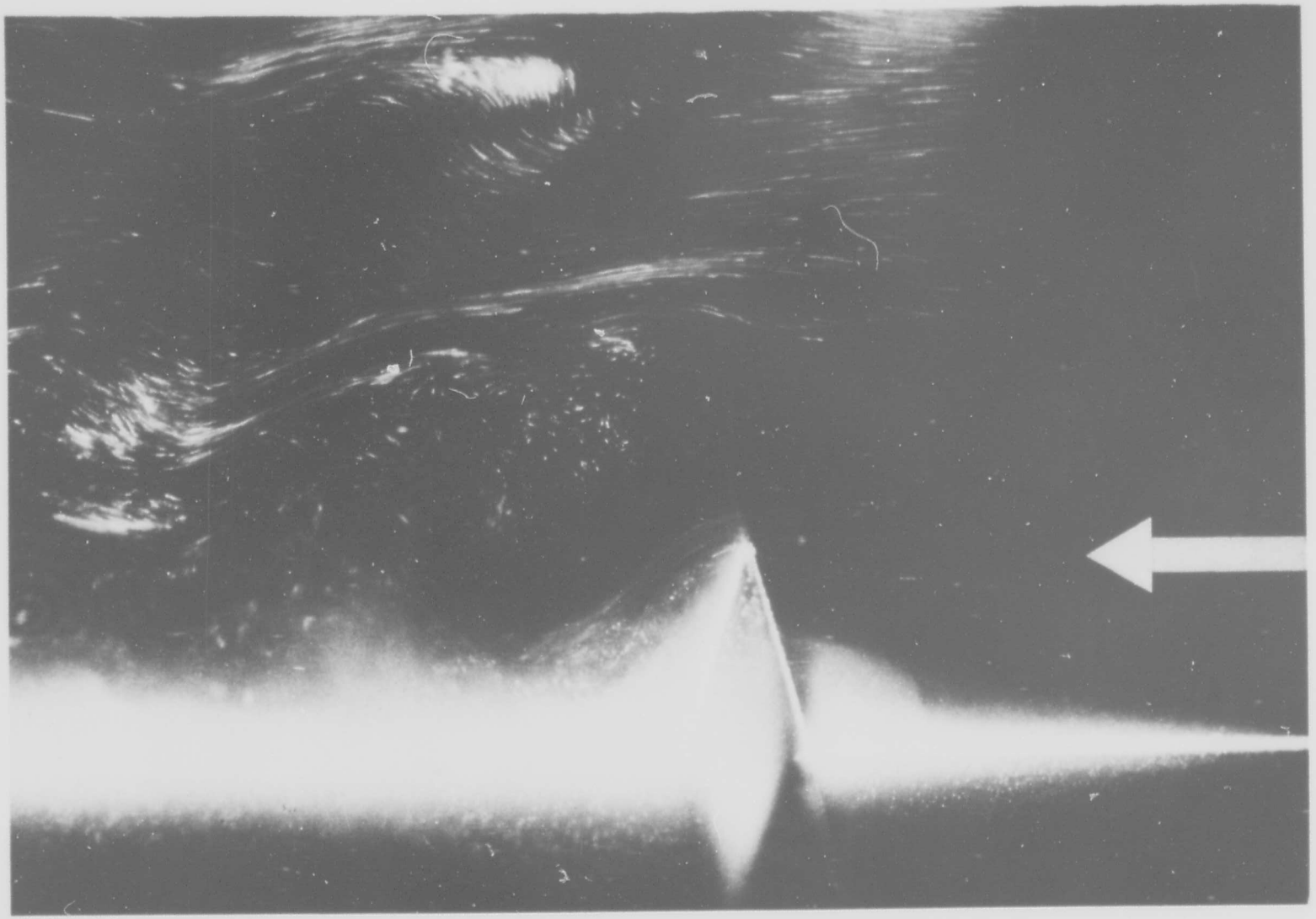

Fig. 5. Lee waves and rotors behind a ridge in a stably stratified flow (Ri=13, Re=914). Upstream velocity and density gradient are constant. (See Fig. 4 caption for other details).

Fig. 6. The eddy behind a ridge in a homogeneous fluid (Re=914). (See Fig. 4 caption for other details.)

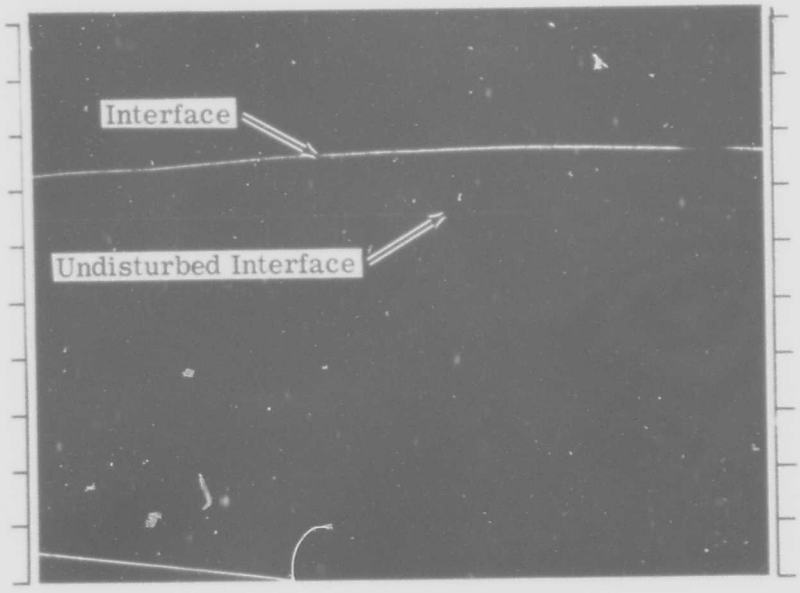

Fig. 7. Internal wave approaching a sloping surface. Upper fluid: white oil, specific gravity = 0.885, viscosity = 13 cp., layer depth = 10.5 in. Lower fluid: water, sp. gr. = 1.0, viscosity = 1 cp., layer depth = 6.5 in. Beach angle = $6^{\circ}40'$.

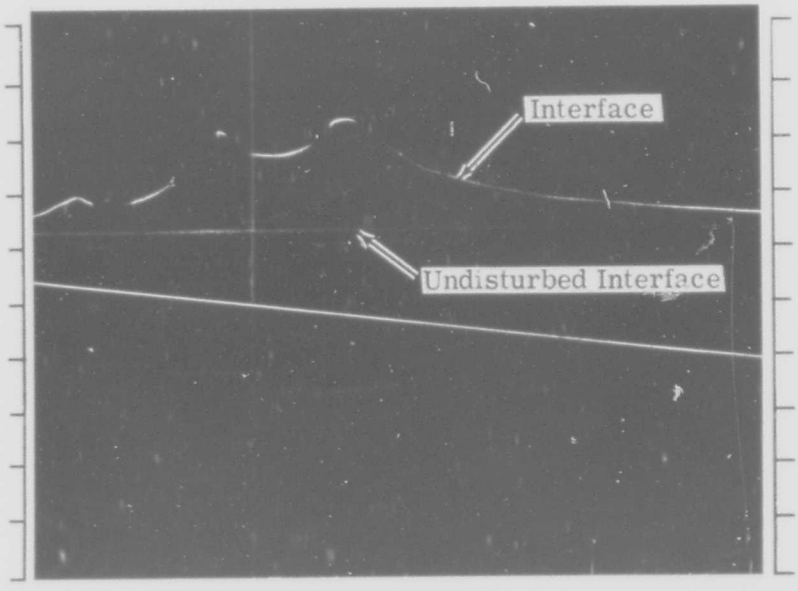

Fig. 8. Breaking of internal wave on a sloping surface. (See Fig. 7 caption for other details.)

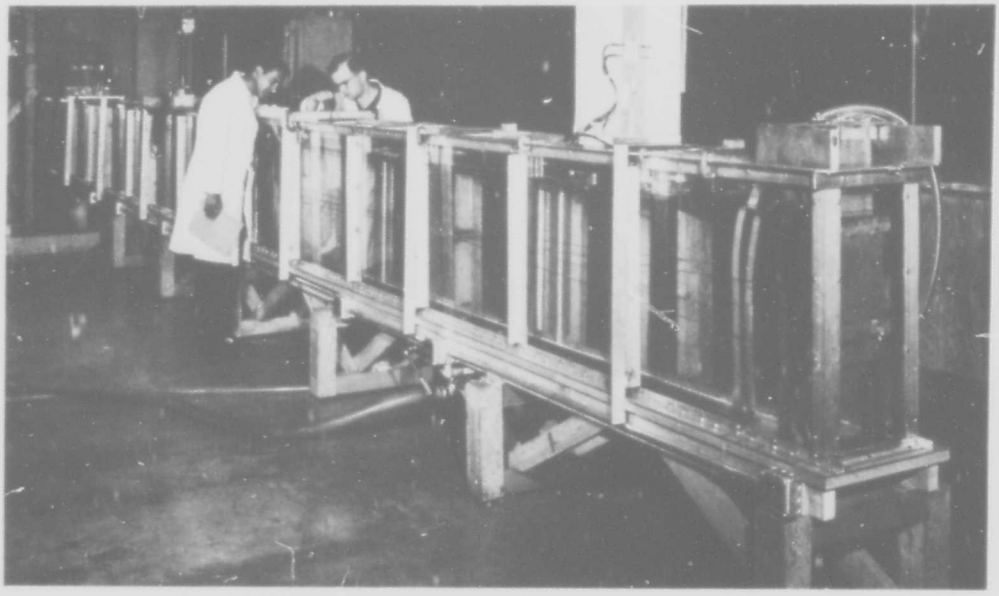

Fig. 9. Towing Tank System B

Fig. 10. The circular cylinder

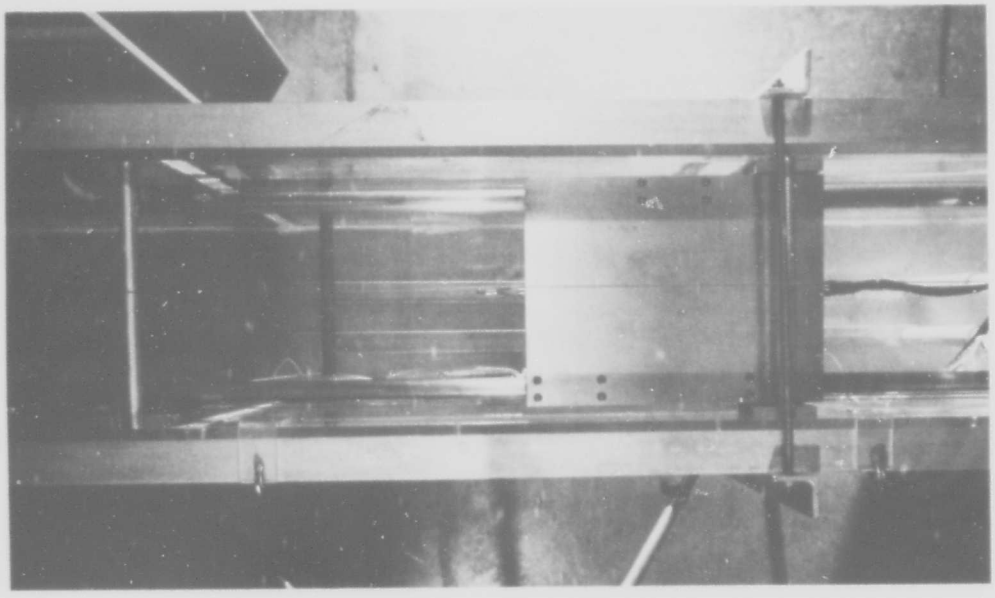

Fig. 11. The air-lubricated probe transport

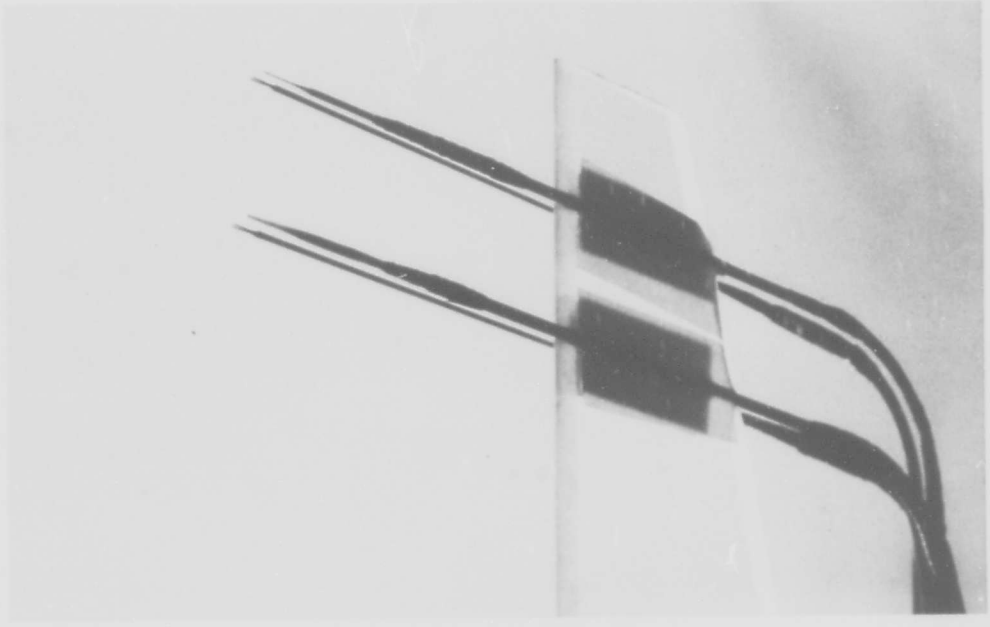

Fig. 12. Hot-film probes and single electrode conductivity probes.

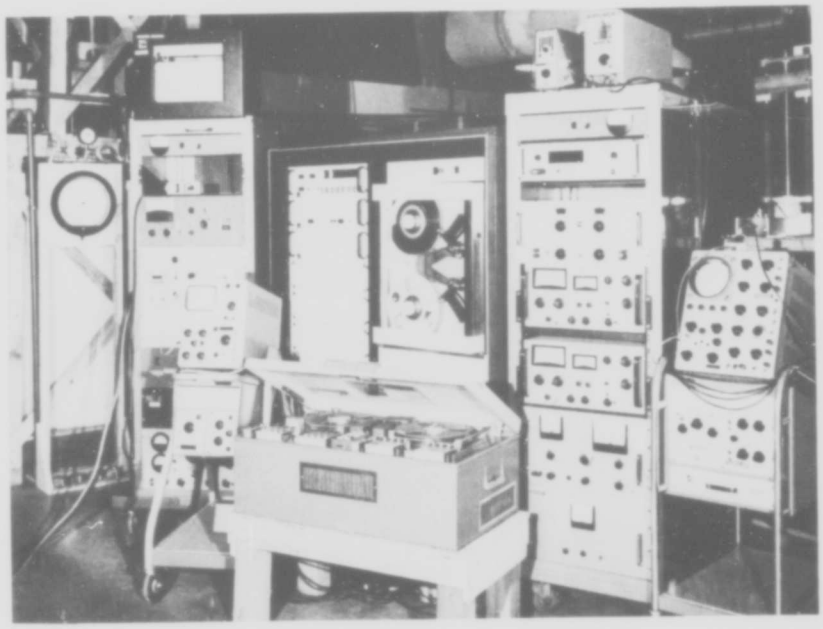

Fig. 13. Instruments and Flow diagram :
(a) Instruments

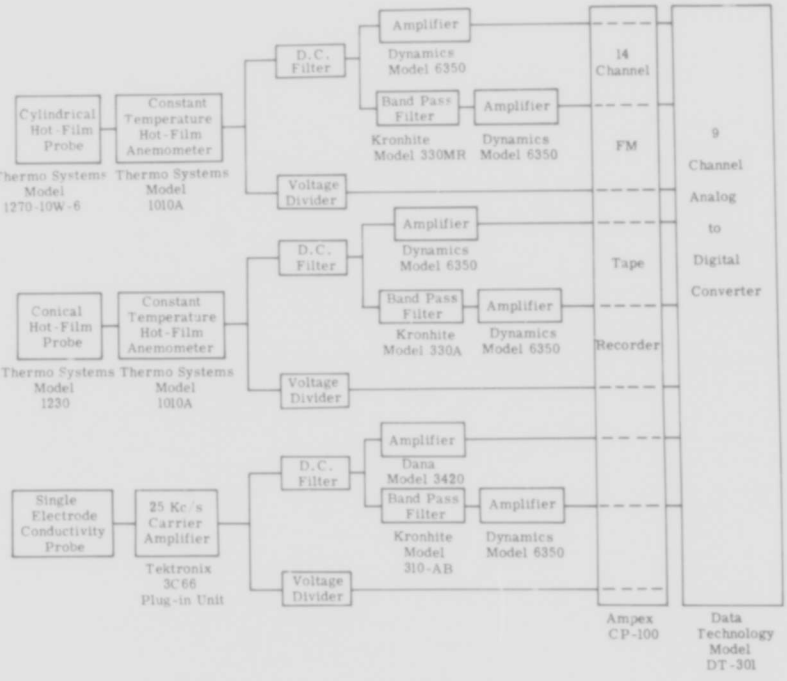

(b) Flow diagram

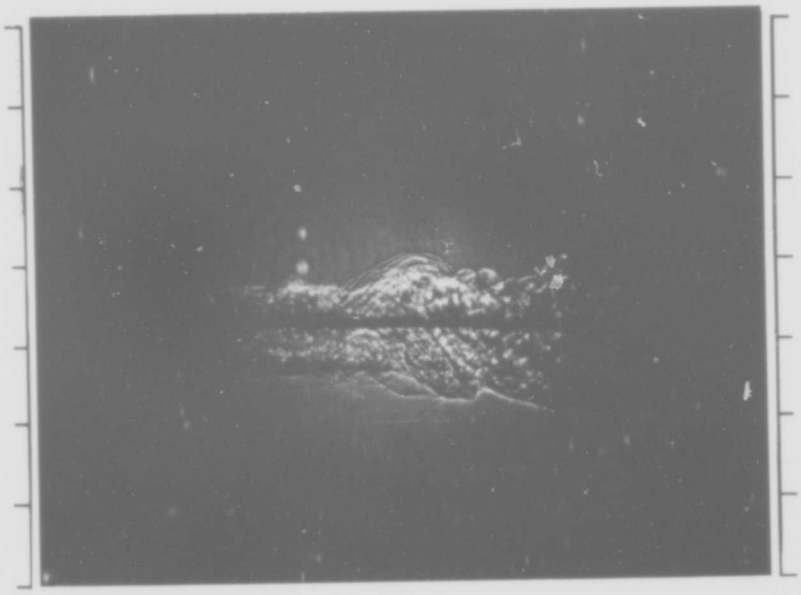

Fig. 14 A shadowgraph picture for the near wake of a circular cylinder in a stably stratified salt water, (Re = 1376, Ri = 0.154), Cylinder diameter = 1.905 cm, Towing speed = 7.226 cm sec^{-1}, Sp. gr. gradient = 2.218×10^{-13} cm^{-1}. Scale: 1 in. per division.

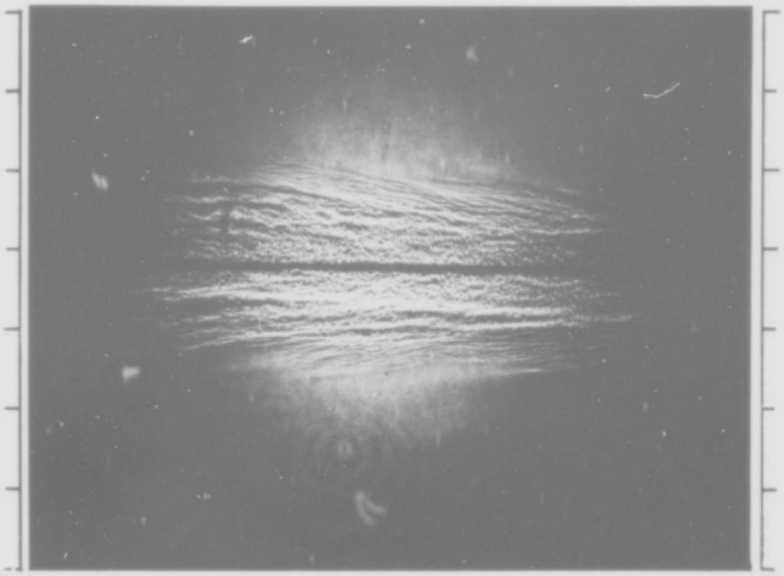

Fig. 15 Shadowgraph pictures for the far wake (Re = 1376; Ri = 0.154).
(a) X/D = 54 at the left edge of the picture

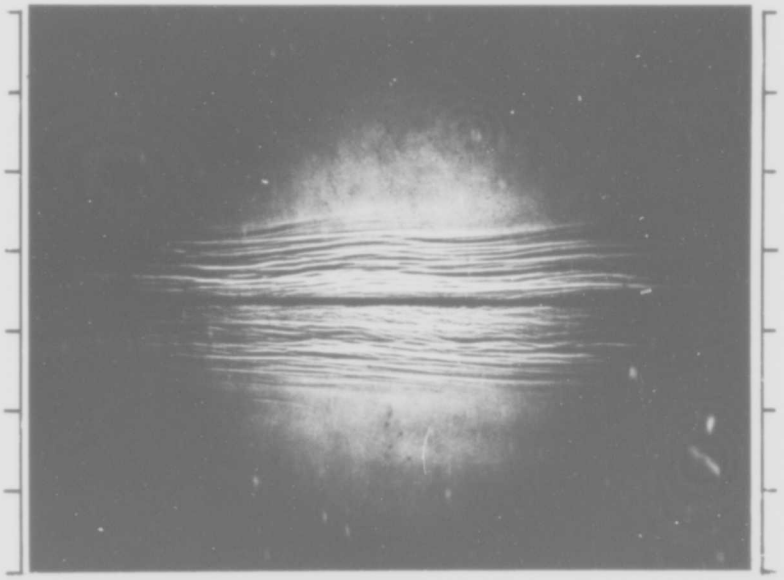

(b) X/D = 110 at the left edge of the picture

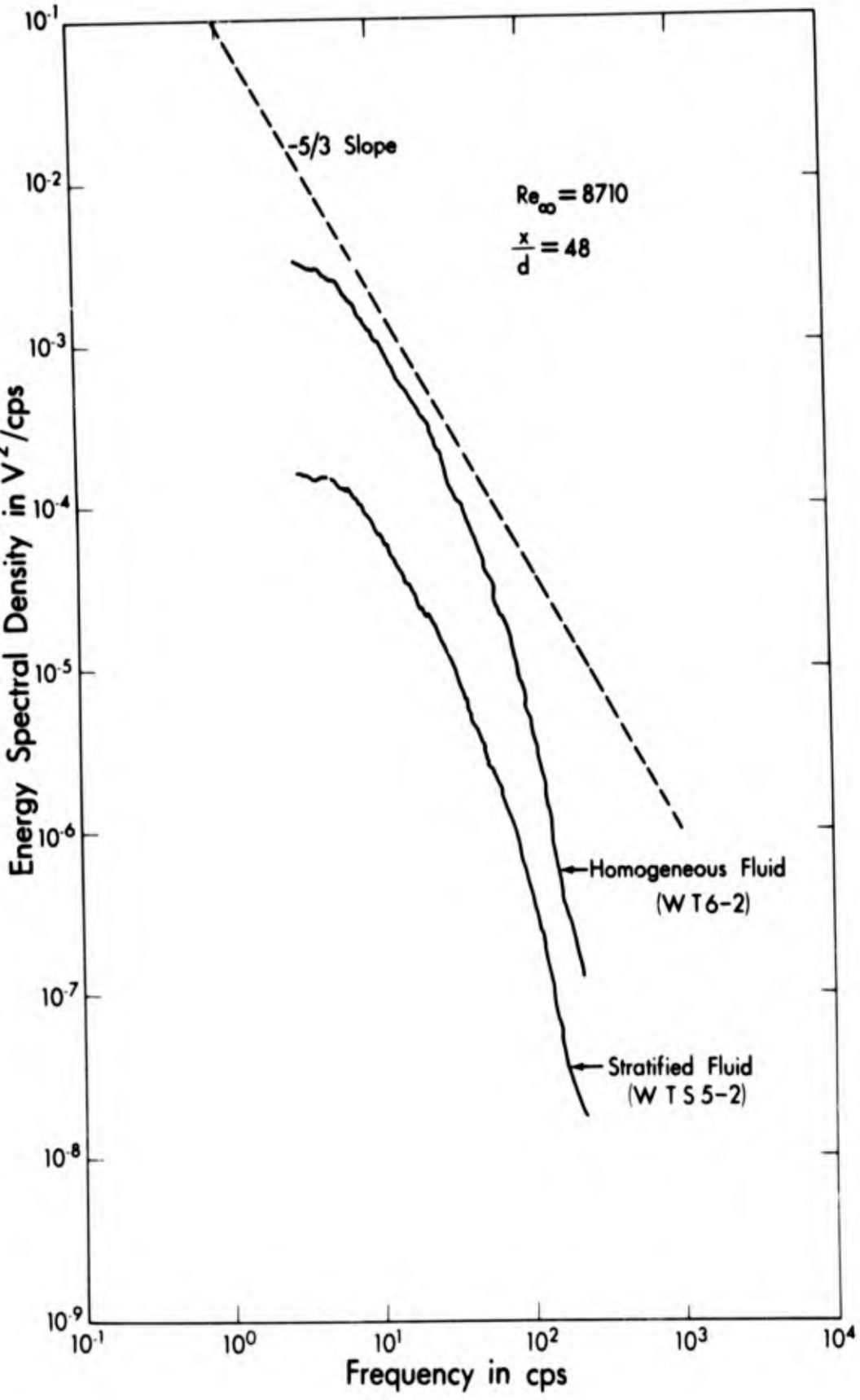

Fig. 16 Comparing the streamwise energy spectra in water with that in stratified salt water, X/D = 48; Cylinder diameter = 1.905 cm; Towing Speed = 42.1 cm sec^{-1}; Sp. gr. gradient = 2.43 x 10^{-3} cm^{-1}; Re = 8030. Ri = .00467.

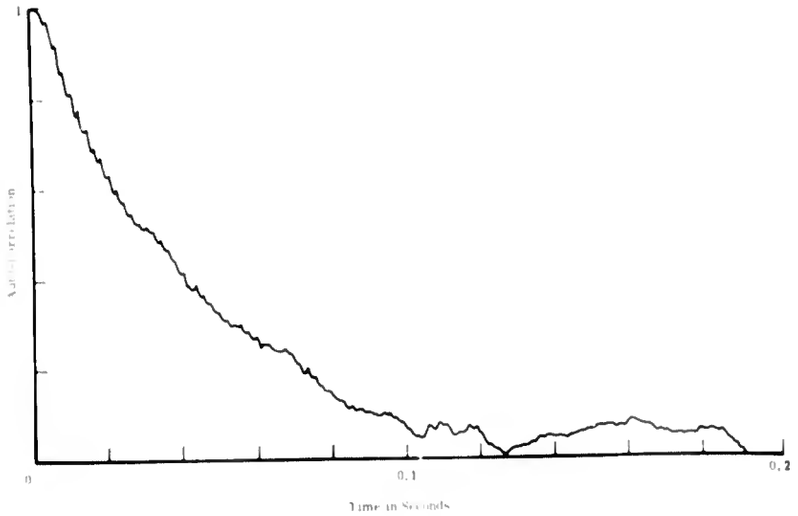

Fig. 17 Streamwise turbulent velocity auto-correlation in a stably stratified fluid. X/D = 48; Cylinder diameter = 1.905 cm; Towing Speed = 45.7 cm/sec; Sp. gr. gradient = 0.731×10^{-3} cm^{-1}; Re = 8710; Ri = 0.00121.

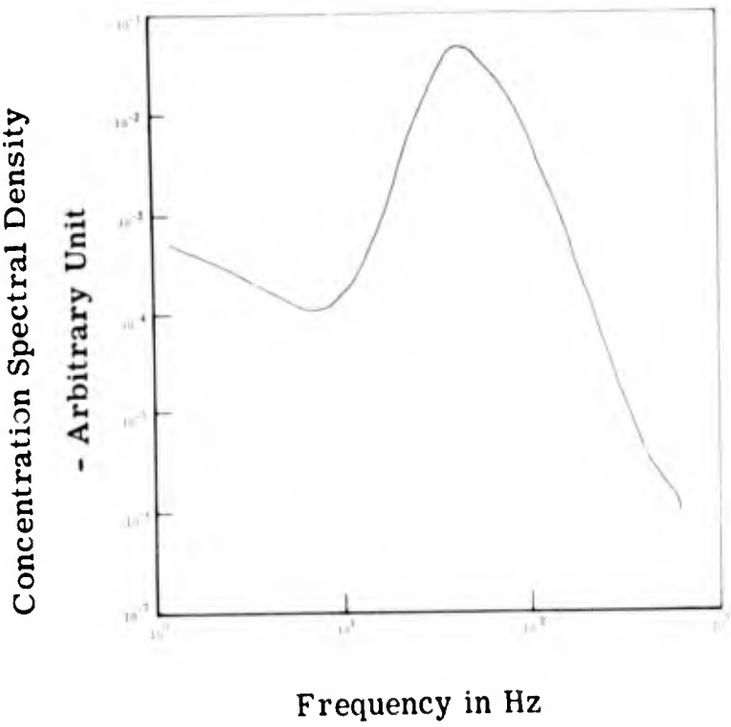

Fig. 18 Concentration spectra in a stably stratified fluid, (See Fig. 17 Caption for other details).

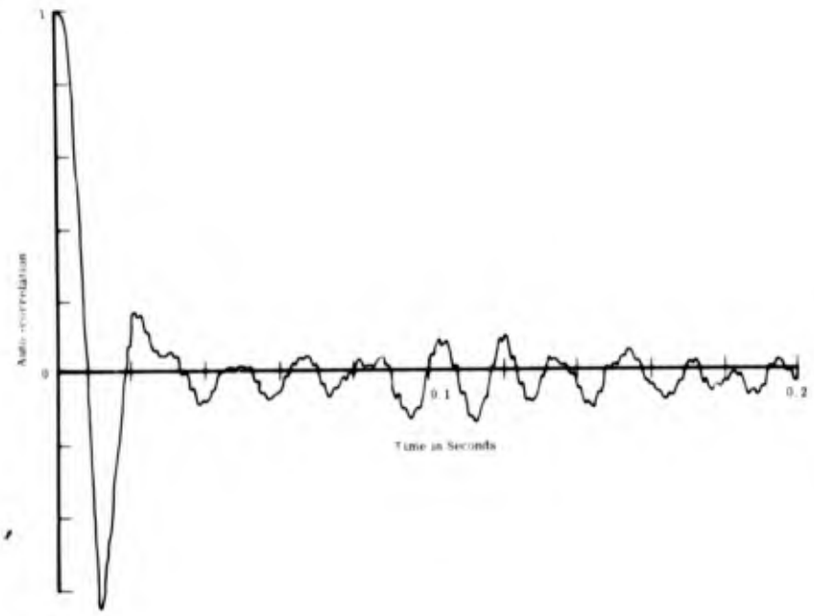

Fig. 19 Concentration auto-correlation in a stably stratified fluid (See Fig. 17 caption for other details).